JOURNAL OF PROPULSION AND POWER
Vol. 23, No. 5, September–October 2007

# Overview on the Aircraft Particle Emissions Experiment

Chowen C. Wey*
*U.S. Army Research Laboratory, Cleveland, Ohio 44135*
Bruce E. Anderson†
*NASA Langley Research Center, Hampton, Virginia 23681*
Changlie Wey‡
*QSS Group, Inc., Cleveland, Ohio 44135*
Richard C. Miake-Lye§
*Aerodyne Research Inc., Billerica, Massachusetts 01821*
Philip Whitefield¶
*University of Missouri–Rolla, Rolla, Missouri 65409*
and
Robert Howard**
*Arnold Engineering Development Center, Arnold Air Force Base, Tullahoma, Tennessee 37389*

DOI: 10.2514/1.26406

**Conducted at the NASA Dryden Flight Research Center during April 2004, the Aircraft Particle Emissions Experiment systematically investigated the gas-phase and particle emissions from a CFM56-2C1 engine on NASA's DC-8 aircraft as functions of engine power, fuel composition, and exhaust-plume age. Emissions parameters were measured at 11 engine power settings ranging from idle to maximum thrust, in samples collected 1, 10, and 30 m downstream of the exhaust plane as the aircraft burned three fuels with different aromatic and sulfur contents. The 1- and 10-m sampling rakes contained multiple gas and particle inlet probes to facilitate a study of the spatial variation of emissions across the engine exhaust plane. Gas-phase emission indices measured at 1 m were in good agreement with the engine certification data as well as with predictions provided by the engine company. However, at low power settings, trace-species emissions were observed to be highly dependent on ambient conditions and engine temperature. Nonvolatile particles emitted by the engine exhibited a log-normal size distribution that peaked between 15 and 40 nm, depending on engine power. Samples collected 30 m downstream of the engine exit plane exhibited a prominent nucleation mode, indicating that secondary aerosols composed of sulfuric acid and low-volatility organic species formed rapidly within the plume as it expanded and cooled. Black carbon emissions were a minimum at approach and a maximum at climb and takeoff engine power settings. Black carbon dominated total mass emissions at high thrust, whereas volatile particles contributed an equal or perhaps greater fraction at low- to midpower settings. Although variations in fuel aromatic content had no discernible impact on particle emissions, volatile particle number and mass concentrations in aged exhaust plumes were highly sensitive to the fuel sulfur content.**

## I. Introduction

THE effect of small-particle emissions on human health and environmental quality has been the focus of recent attention from the scientific community and environmental regulatory agencies. Particles suspended in the atmosphere have various potential effects on humans and the environment, including local air and water quality and global climate change. In recent years, it has become increasingly evident that very small particles [i.e., with diameters of submicrometers (submicrons)] are of particular concern, due to their efficiency in either scattering or absorbing solar radiation and their role in the formation of clouds, depending on particle type. They also appear to be a crucial element in understanding human health responses to air pollution. The majority of particles emitted by aircraft engines are fine particles with diameters of less than 400 nm .

Although similar particles are generated by many sources, such as various industrial, power generation, and transportation activities, the emissions from aircraft occur primarily in and around airports or airfields and along flight paths. At cruise altitudes, aircraft are a unique source for directly depositing small nonvolatile particles to the atmosphere. Whether aircraft-generated particles are unique in other respects has yet to be unequivocally determined. Currently, the characteristics of aircraft particle emissions are one of the least understood and quantified relative to those from other major pollution sources. In addition, they are also the least understood and quantified among all emissions from aircraft engines.

Over the past decade, NASA has sponsored a variety of studies to gather detailed aircraft emission data to assess the environmental impact of aviation and to develop ultraefficient and low-emission turbine engine technology [3–8]. An important recent study was the Aircraft Particle Emissions Experiment (APEX), which was conducted at NASA Dryden Flight Research Center (DFRC), Edwards Air Force Base, California in April 2004. Particle and gas-phase emissions from one of the NASA DC-8 aircraft's CFM56-2C1 engines were measured as functions of engine power, fuel composition, and exhaust-plume age. The mission's scientific objectives included 1) establishing the engine's particle and trace-gas emission indices as functions of engine power, 2) determining

Received 9 July 2006; revision received 10 January 2007; accepted for publication 28 March 2007. 

*Aircraft Particle Emissions Experiment Project Scientist, Mail Stop 60-2, 21000 Brookpark Road.
†Senior Research Scientist, Mail Stop 483, 21 Langley Boulevard.
‡Senior Research Engineer, Mail Stop 5-10, 21000 Brookpark Road.
§Principal Scientist and Director of Aerothermodynamics, 45 Manning Road.
¶Professor and Chair of Chemistry, Director of University of Missouri–Rolla Center of Excellence, G-7 Norwood Hall.
**Engineer Specialist, 1099 Schriever Avenue.

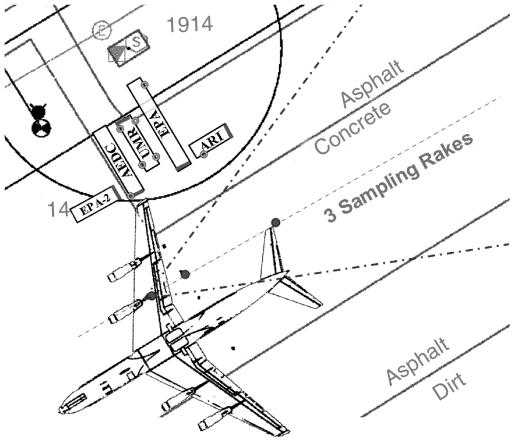


**Fig. 1 Test field layout showing the positions of the aircraft, instrument trailers, and sampling probes (dots). The NASA particle measurement system and the central sample distribution manifold are located in the EPA trailer. NASA gas-measurement systems are located in the Arnold Engineering Development Center (AEDC) trailer.**

the impact of fuel sulfur and aromatic content on soot and secondary particle formation, 3) observing the evolution of particle characteristics and chemical composition within the engine exhaust plume as it cooled and mixed with background air, and 4) determining the spatial variation of particle properties across the engine exhaust plane. APEX also provided an opportunity to evaluate new measurement and sampling techniques for characterizing aircraft gas and particle emissions. A detailed description of the experiment plan, along with data tables and reports from participating researchers, is presented by Wey et al. [8]. Papers presenting detailed results from several participating groups are included in the special section of this issue. This document provides an overview of the experiment and summarizes important observations and results.

## II. Experiment

To conduct the emission tests, the NASA DC-8 aircraft was chocked on a concrete testing pad adjacent to a taxiway at Edwards Air Force Base near the NASA DFRC hanger. Figure 1 shows a diagram of the experiment layout. Instrument trailers were parked on the right side of the aircraft, about 25-m outboard of the test engine. Gas and particle sampling probes were positioned 1, 10, and 30 m downstream from the exhaust plane of the aircraft's right inboard engine. It was expected that engine exhaust would be mixed with the ambient air to an approximately 1:10 ratio at 10 m and 1:30 ratio at 30-m downstream locations [7]. As shown in Fig. 2, 1- and 10-m probe rakes held six particle and six gas-sampling probes to facilitate a study of the spatial variation of emissions across the engine exit plane. The particle inlet probes were designed to allow the introduction of a concentric flow of dilution gas (dry $N_2$) just downstream of the probe tip. Six additional large-diameter gas inlet probes were attached to the outside of the 1-m rake to meet the demands of a few high-flow instruments. Because we expected the plume to be relatively dilute at 30 m, the probe located at this position sampled the aged exhaust plume without further dilution. A portable weather station was erected a short distance from the test site that continuously monitored and recorded ambient wind, temperature, and pressure. Engine fan speed was defined for each thrust level and used to set engine operations. However, it was decided to allow the fan speed drift, following the varying ambient conditions. Engine operating parameters including fan speed, core speed, exhaust temperature (near the end of nozzle), and fuel flow rate were read from the airplane cockpit panel and recorded manually. Fuel flow rate was chosen to be the engine parameter to correlate with emissions because it reflected engine operation conditions and was the most commonly used parameter to calculate emissions [9].

Three different fuels were employed during APEX to examine the impacts of fuel sulfur and aromatic contents on gas and particle

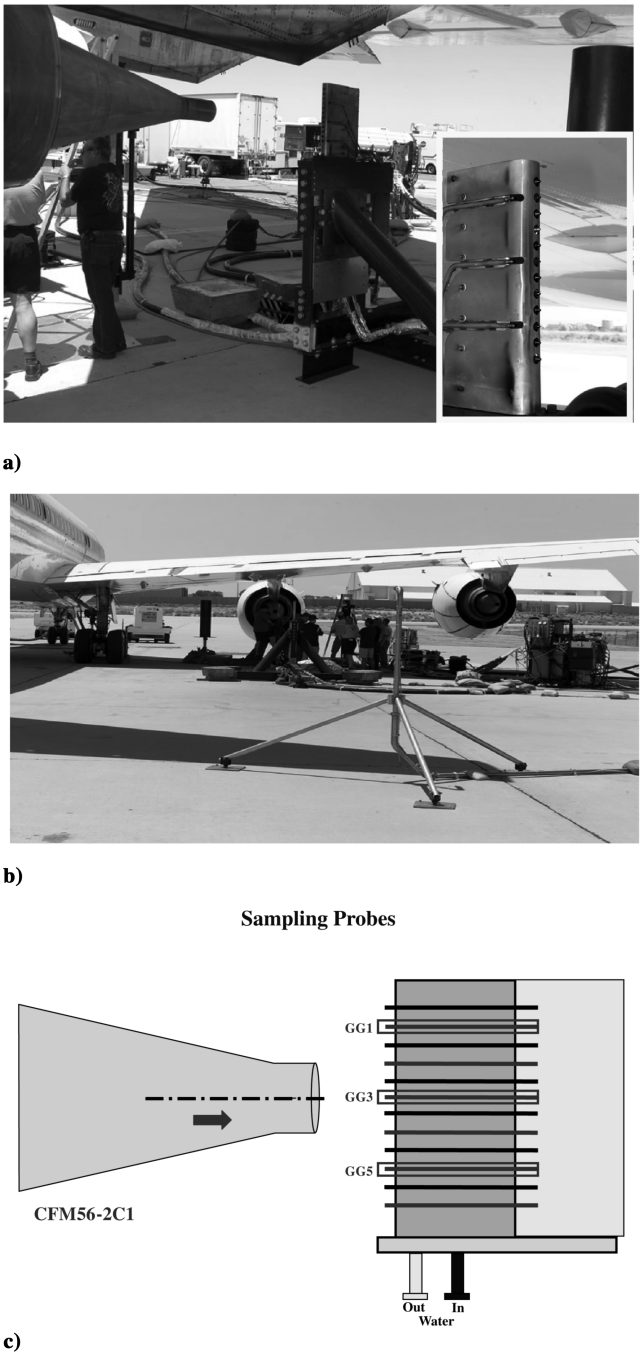


**Fig. 2 Photo of 1-m sample stand (top), in which the right corner inlay shows the 1-m sample rake with 6 gas, 6 particle, and 6 external sample probes; photo of 1-, 10-, and 30-m sample stands (middle) behind the aircraft engine, in which the 30-m sample stand has a single probe; and schematic of the 1- and 10-m sample rakes (bottom).**

emissions. The base fuel was standard JP-8 supplied by the Edwards Air Force Base fuel dump that contained 383 ppm by mass (ppmm) of sulfur and 17.6% (by volume) aromatic compounds. The high-sulfur fuel was produced by mixing a large aliquot of tertiary butyl disulfide into a tanker truck containing base fuel to raise the fuel sulfur content to 1595 ppmm. Producing the high-aromatic fuel following the same approach would have required a large amount of aromatic additive and hence would have been cost-prohibitive. Thus, high-aromatic fuel was obtained by surveying the aromatic contents of fuels available from California refineries and selecting a jet A that contained 530 ppmm of sulfur and 21.6% aromatic species [10].

Two different engine test matrices were used during APEX. The NASA test matrix was designed to investigate the effects of engine

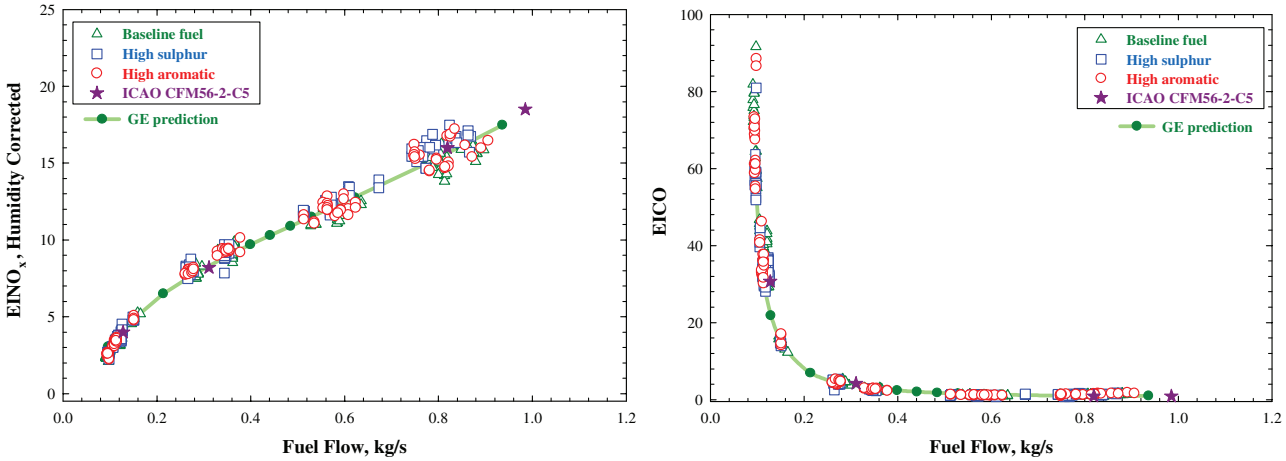


**Fig. 3 Functions of engine flow rate at 1 m; measured data are in good agreement with the ICAO certification data and the engine company's predictions.**

operating parameters on emissions. It included 11 power settings: 4, 5.5, 7, 15, 30, 40, 60, 65, 70, 85, and 100%. With the concerns of operating a parked aircraft at 100% thrust, the maximum thrust was restricted to approximately 93%, but is still labeled as 100% in this paper. Except for the 100% thrust level for which run time was limited to 1.5 min, approximately 4 min were spent at each power setting to allow adequate time for analyzing samples from each of the three downstream probes. The Environmental Protection Agency (EPA) test matrix followed the International Civil Aviation Organization (ICAO)-defined landing–takeoff cycle to generally simulate aircraft emissions at the airport and consisted of approximately four repetitions of 26 min at idle (7%), 0.7 min at takeoff (100%, also restricted to approximately 93%), 2.2 min at climb (85%), and 4 min at approach (30%) power settings. It is important to note that in practice, the times in mode are typically different from the ICAO-defined values and depend on various parameters such as aircraft/engine model, airplane usage (e.g., cargo/passenger and flight range), airline/airport operations, etc.

A large array of state-of-the-art instruments were deployed to characterize gas and particle emissions from the CFM56-2C1 engine. Using a standard suite of conventional gas analyzers (CGA), certification gas concentrations including carbon monoxide (CO), carbon dioxide ($CO_2$), nitrogen oxides ($NO_x$), and total hydrocarbons (HC) were measured. A Fourier-transform-infrared multigas analyzer (MGA) was also fielded for both evaluation purposes and to measure nitrous oxide ($N_2O$), sulfur dioxide ($SO_2$), and speciated hydrocarbon concentrations [11]. A tunable infrared laser differential absorption spectrometer (TILDAS) [12] and a proton-transfer-reaction mass spectrometer (PTR-MS) were deployed [13] to measure nitrous acid (HONO), $N_2O$, $SO_2$, and a number of hydrocarbon species. A smoke meter to determine the engine's smoke number using the approach recommended for engine certification tests was deployed. The concentration and microphysical properties of particle emissions (size distribution, solubility, and volatility) were measured using condensation particle counters (CPCs) [14], scanning mobility particle sizers (SMPSs) [14], a particle soot absorption photometer [14], and a differential mobility spectrometer (DMS) [15]. Particle nonrefractory chemical compositions and chemically speciated size distributions were measured using an aerosol mass spectrometer (AMS) and determined black carbon emission indices using a multi-angle aerosol photometer (MAAP) [16]. A tapered element oscillating microbalance (TEOM) was fielded to determine total particle mass emissions. An experimental multi-angle optical scattering instrument was deployed to determine particle mass for test and evaluation purposes. APEX was also used as an opportunity to test and evaluate various methods of collecting particle filter samples for offline analysis.

The EPA brought a suite of instruments that were originally used for on-road diesel testing, including a CPC, SMPS, TEOM, and an electrical low-pressure impactor to measure particle physical and chemical properties. EPA's data are not yet publicly available and hence will not be presented in this paper. However, data acquired by other team members under both NASA and EPA test matrices are presented.

## III. Summary of Results

APEX was the first ground-based experiment to simultaneously examine the gas-phase and particle emissions from a commercial-class aircraft with turbofan engines over the complete power range of its engines. As such, a great deal of new information was obtained, including observations regarding exhaust mixing and dynamics. Although the 1-m sampling rake was carefully positioned to align its probes with the core exhaust flow, samples drawn from the top gas probe were sometimes mixed with 5 to 10% fan air. Similar variations at the top three gas probes were observed from the 10-m rake, but higher proportions of fan air were sometimes mixed in the samples because of the strong ambient wind. Gas emissions measured from the 10-m rake exhibited the same trend as those from the 1-m rake, but concentrations were typically an order of magnitude lower, due to the entrainment of bypass flow. Thus, the 10-m data exhibited higher variability than similar data recorded behind the 1-m probe.

### A. Gas-Phase Emissions

Reference [17] archives data from engine exhaust emissions certification tests conducted in accordance with various national authority regulations that are based upon the standards and recommended practices prescribed by the ICAO under Annex 16, Volume 2 of the Chicago Convention. We found that $NO_x$ and CO emissions measured from the 1-m rake, expressed as emission indices [(EIs), defined as grams of species per kilogram of fuel] of CO and $NO_x$ and EICO and EINO$_x$, were in good agreement with ICAO certification data for the CFM56-2C5 (data were not available for the C1-series engine) and predictions from cycle calculations performed by the engine company (Fig. 3). EICO increased when EINO$_x$ decreased, as expected. The nitrogen dioxide ($NO_2$) fraction of $NO_x$ varied from about 70% at idle to about 9% at maximum power [10]. HC emissions had the same trend as CO and also were in good agreement with ICAO certification data and the engine company's predictions. Although exhibiting much higher values at idle, EIHC decreased by more than two orders of magnitude and were almost negligible above 15% engine power. EIHC depends strongly on engine combustion conditions; for example, ambient temperature affects combustor inlet temperature and hence HC emissions. In addition, HC levels were approximately a factor of 2 higher just after a cold engine start; evidence for this effect was observed throughout the APEX project (Fig. 4). Similar effects were noted in the engine

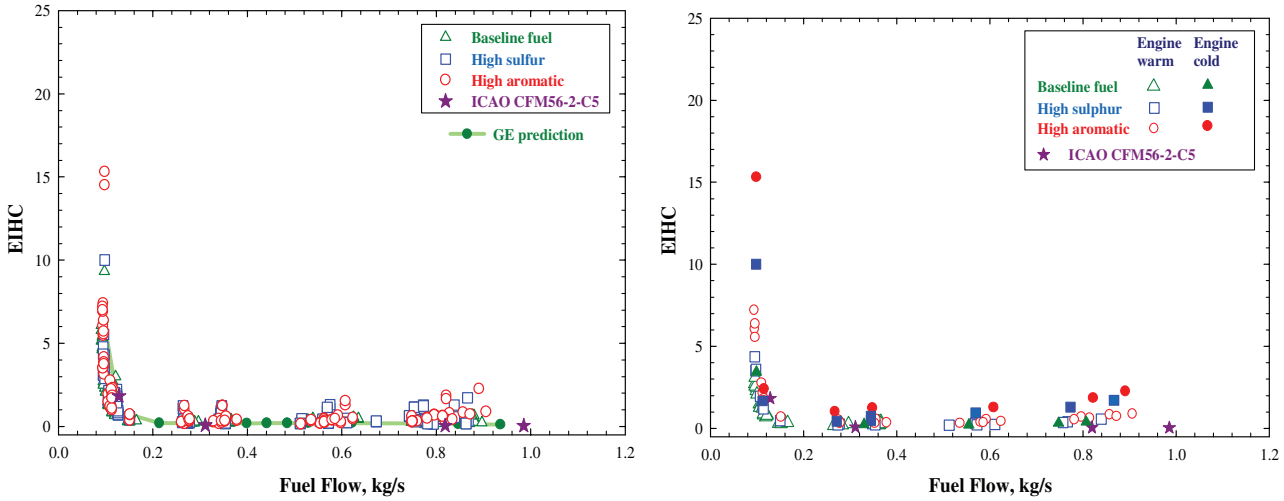


**Fig. 4 EIHC as a function of engine flow rate (left) and effect of engine temperature on EIHC (right); data are from the second top gas probe of the 1-m rake.**

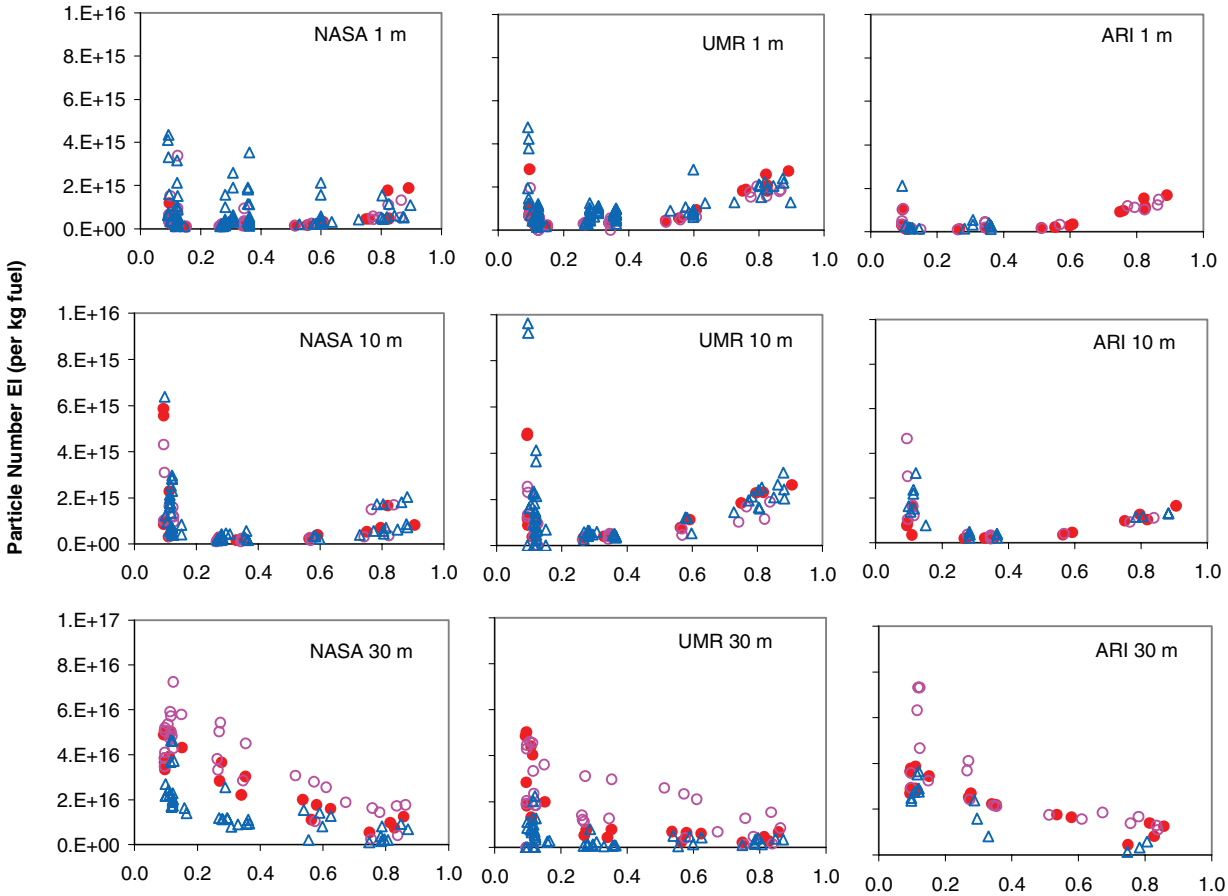


**Fig. 5 EIn measured by the NASA CPC (left column), UMR DMS500 (middle column) and the ARI CPC (right column) as functions of fuel flow rate at three sampling locations using three types of fuel.**

company's early emissions variability testing of CF6-50 engines.[††] When plotted as a function of fuel flow rate, the EI for higher-molecular-weight hydrocarbons measured by TILDAS and PTR-MS correlated with those of formaldehyde (HCHO).

$SO_2$ and a variety of light hydrocarbons were measured by MGA. However, much higher uncertainties should be applied when using these data. $SO_2$ concentrations varied directly according to fuel sulfur content. More than 90% of fuel sulfur content was converted to $SO_2$ with a high uncertainty level [11].

### B. Particle Emissions

For total particle emissions (Figs. 5–7), we noted that at 1 m, emitted particles were log-normally distributed within a single mode and ranged from a few nanometers to over 300 nm in diameter [15]. At 30 m, particle distributions typically exhibited two distinct modes, one corresponding to nonvolatile particles and peaking at roughly the same diameters observed in the 1-m samples and the other occupied

[††]Data available online at http://particles.grc.nasa.gov/ [retrieved 23 July 2007].

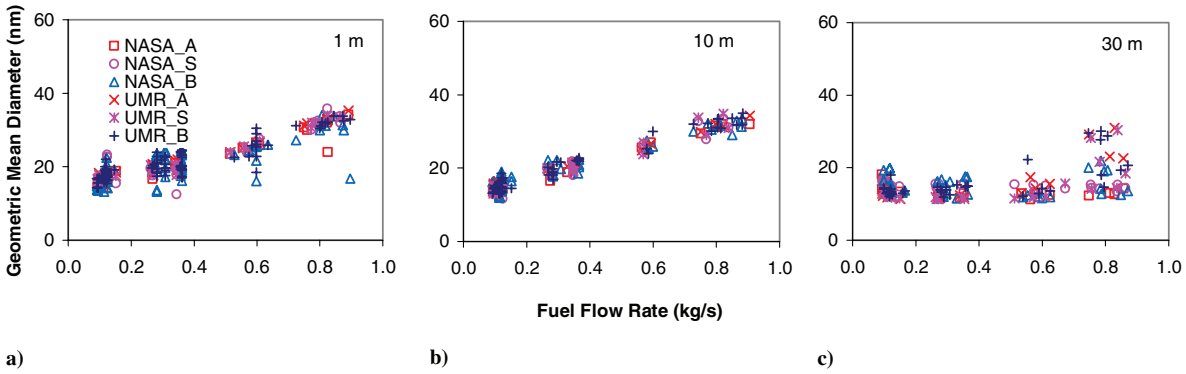


**Fig. 6 Particle geometric mean diameters measured by the NASA SMPS and the UMR DMS500 as functions of fuel flow rate using three types of fuel.**

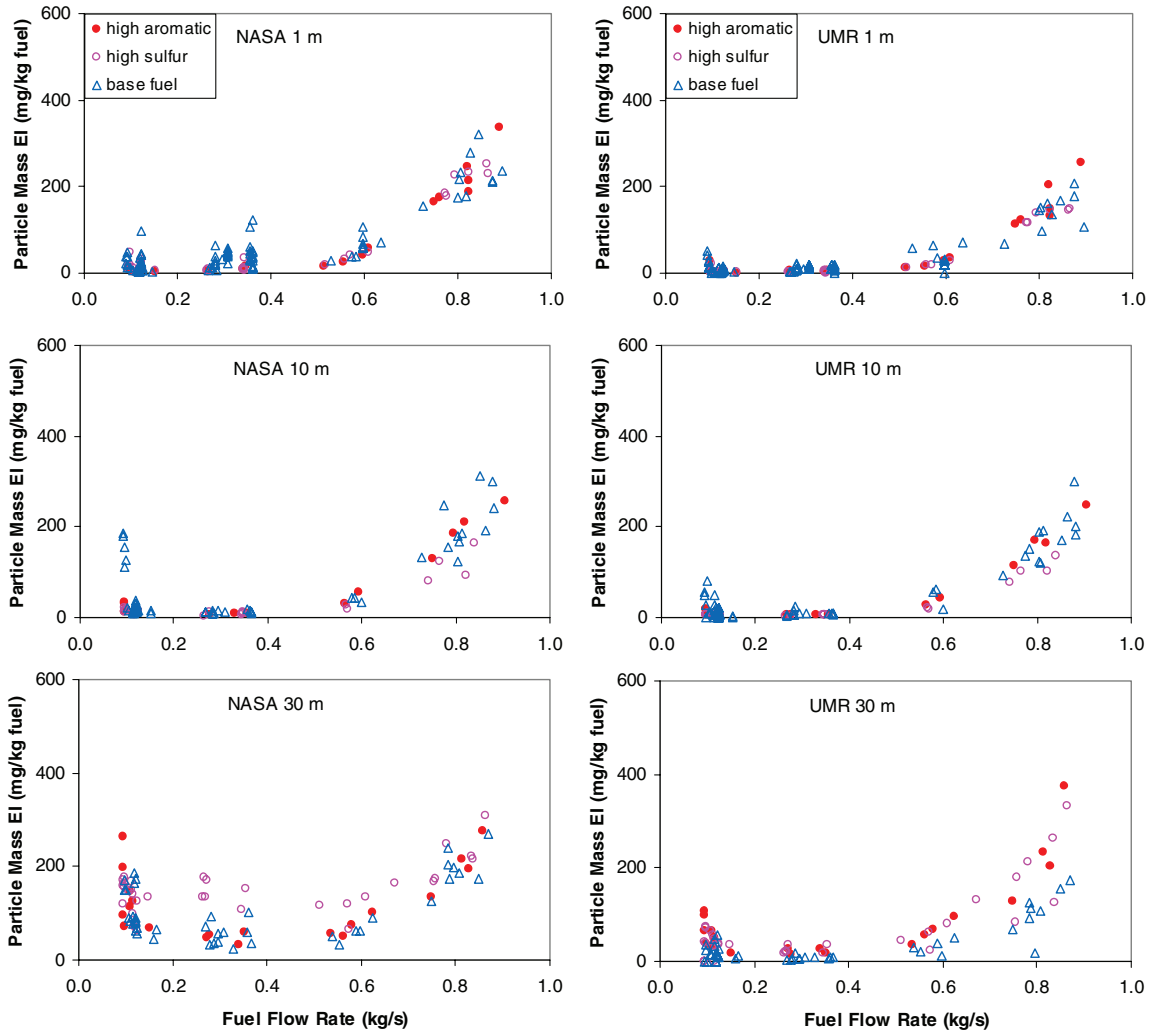


**Fig. 7 EIm measured with the NASA SMPS (left column) and the UMR DMS500 (right column) as a function of fuel flow rate using three different fuels; values are calculated using a particle mass density of 1 $g/cm^3$.**

by freshly nucleated sulfur and organic particles peaking at less than 12 nm. It is not clear whether these new particles formed within the expanding plume or during the ~6-s samples spent within transport tubing before being analyzed or possibly some combination of the two [16].

Total particle number-based emission indices (EIn) ranged from less than $1 \times 10^{15}$ particles/kg of fuel at 1 m to $6 \times 10^{16}$ particles/kg of fuel at 30 m. At the 1- and 10-m locations, total particle EIn reached a minimum at medium power levels. At the 30-m location, total particle EIn values were greatest at idle, then monotonically decreased with increasing thrust. At 30 m and for all fuel types, under low-ambient-temperature conditions, a nucleation mode was observed with a mean diameter at or below 10 nm. Total particle EIn values were typically 5 to 20 times greater at the 30-m sampling location than at 1 m, indicating that large numbers of new particles formed [14].

Significant variations were found in EIn measured across the diameter of the engine exhaust at the 1-m location [15]. At a given power setting, particle EIn measured within samples from the plume edge were often 10 times higher than those from the center of the exhaust plume. One potential explanation is that substantial particle nucleation occurred within samples pulled from the exhaust-plume

edge, for which the temperature was colder and exhaust was more diluted by ambient air. Other potential factors include, but are not limited to, the distribution pattern across the exhaust, recirculation of aged aircraft emissions into the bypass flow, and variations in sampling procedures. Changes in ambient temperature introduced significant variability in the engine's primary particle emissions [14]. Plotting the EIn as a function of fuel flow rate instead of engine power (which varies with inlet temperature) explains some, but not all, of this variability.

Particle mass and black carbon emission indices (EIm and $EIm_{BC}$, respectively) were a minimum at low powers and increased with power, reaching values more than 0.3 g of particles/kg of fuel at power levels higher than 85% [14–16]. At high engine powers, particle mass emissions were dominated by black carbon at all sampling locations. At low power settings, the sulfate component was negligible at 1 m, but accounted for 20% or more of the total mass at 30 m, depending on the sulfur content of the fuel being burned. Organic particles also contributed a significant mass fraction to samples collected at 30 m. The volatile particle fraction clearly increased with plume age, accounting for 50% to greater than 90% of total number and 40 to 75% of total mass at 30 m, depending on engine power settings and fuel composition [14].

Nonvolatile particle (presumably black carbon) emissions were log-normally distributed in a single mode, with individual particles ranging from 3 to over 300 nm in diameter. The geometric mean diameter increased roughly linearly with power, ranging from around 15 nm at idle to about 40 nm at maximum power. Nonvolatile particle EIn varied from 0.16 to $3 \times 10^{15}$ particles/kg of fuel, and were greatest at idle and takeoff thrust settings and were a minimum at power levels corresponding to approach. For low power settings, nonvolatile particle EIn decreased over time as both engine and ambient temperatures increased. Nonvolatile particle size as well as EIn and EIm were independent of fuel properties or downstream sampling distance (plume age). EIm values were nonlinearly dependent on engine power and typically less than 20 mg of particles/kg of fuel over the 4 to 70% engine power range and greater than 200 mg of particles/kg of fuel at and above 85% power level [14,15].

Samples collected further downstream of the engine exhaust plane often contained large numbers of particles that evaporated at temperatures below 300°C [14]. For these volatile particle emissions, we found that at 30 m, size distributions often exhibited a prominent nucleation mode, particularly in the medium to low engine power cases. This dominance of small particles resulted in geometric mean diameter values of smaller than 15 nm for all power settings, although the distribution is distinctly bimodal, especially at the highest powers. Although readily apparent at the 30-m sampling location, volatile particles were not observed at 1 m and were barely detectable in the 10-m samples. In aged plumes, along with forming new particles, low-volatility hydrocarbons and sulfur condensed onto the surface of nonvolatile particles, increasing their diameter and, potentially, their water solubility. In addition to sulfur, hydrocarbon species accounted for a significant fraction of volatile particle mass at the 30-m sampling location, particularly at low engine power settings. At the 30-m sampling location, volatile particle EIn were 5 to 20 times greater than nonvolatile particle EIn and strongly dependent on fuel sulfur content, being substantially enhanced in high-sulfur fuel test series. Volatile particle EIn decreased with power, which may reflect a lower production of aerosol precursors at higher engine power settings or simply a shift in the equilibrium between new particle formation and condensation of precursors onto existing particle surfaces. Volatile particle EIn also depended on sample age and dilution history and ambient temperature. At 30 m, nonvolatile particle EIn increased, whereas volatile particle EIn decreased with engine power; the sum of these trends produced an overall decrease in EIn with increasing engine power.

At higher engine power settings, black carbon was the dominant component in particulate samples collected from all inlet probes. At 30 m and at lower power settings, sulfate and organic aerosols accounted for a majority of total particle mass emissions. The condensed sulfate EI varied only a modest amount within experimental uncertainty as power varied, whereas the condensed organic EI increased significantly at powers close to idle under operating conditions that also produced enhanced unburned hydrocarbons and CO EIs.

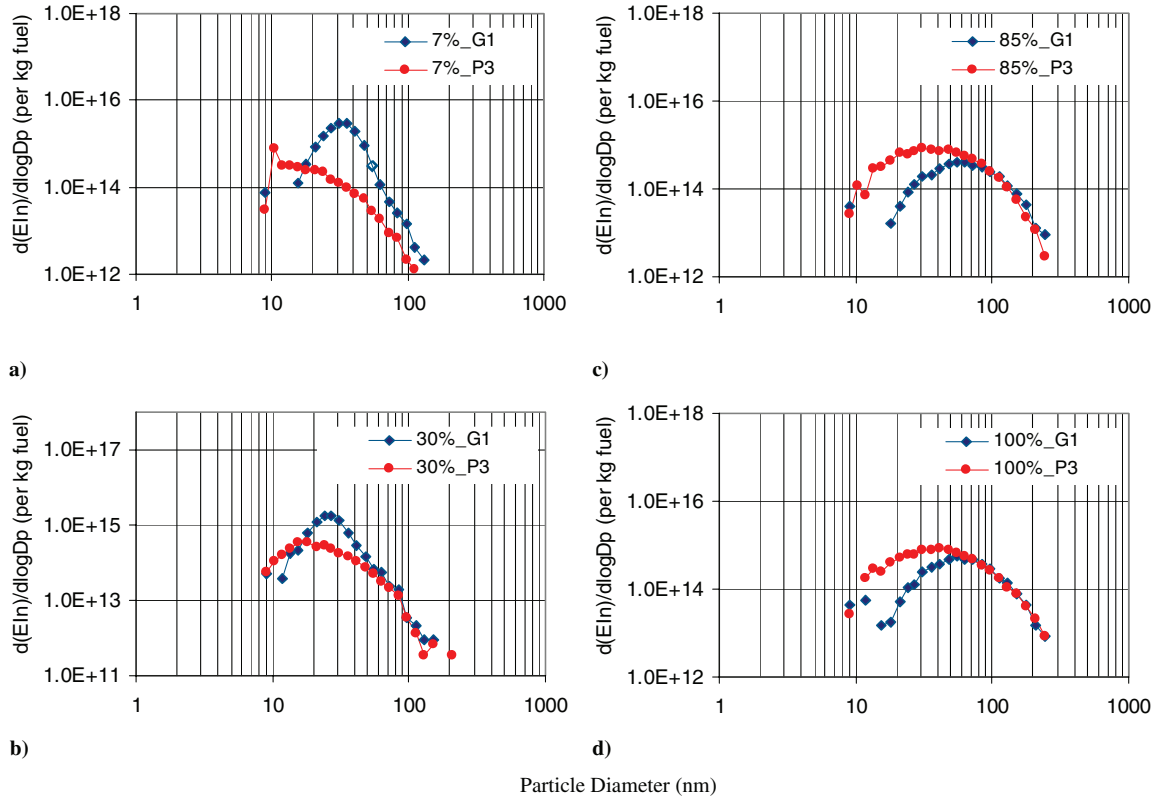


**Fig. 8 Particle size distributions measured by NASA from gas probe G1 and particle probe P3 at 1 m on 20 April with high-sulfur fuel.**

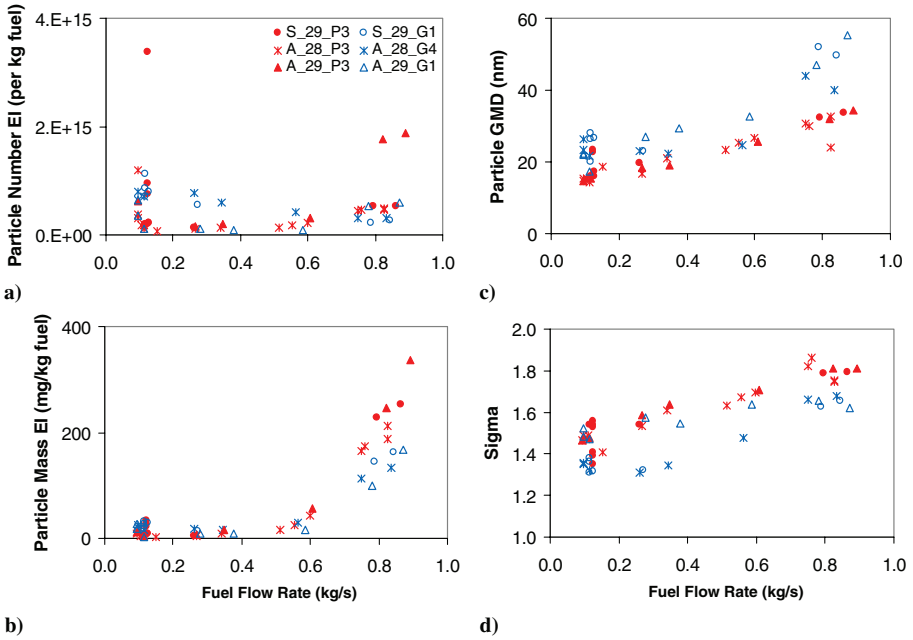


**Fig. 9 Particle properties measured by NASA from gas probes G1 and G4 and particle probe P3 at 1 m on 28 and 29 April with high-aromatic fuel A and high-sulfur fuel S. When sampled from gas probes, exhaust sample dilutions were added at the sample distribution manifold.**

A major issue in investigating aircraft particle emissions is whether standard gas-sampling probes deliver representative samples or if probes that provide dilution air just downstream of the inlet tip are needed. Figure 8 shows that at the 1-m sampling location and for any given power setting, particle size distributions are significantly different in samples drawn through standard gas inlet probes attached to heated lines (to which dilution air was introduced about 15 m downstream of the probe tip) from those in samples collected from aerosol probes to which four- to tenfold concentric dilution was added near the inlet tip. EIn, EIm, and particle geometric mean diameter values were all substantially different in samples acquired from the gas and particle probes (Fig. 9). The enhanced nucleation, coagulation, and overall transport losses that occurred within the gas-probe system caused its EIn and EIm values to vary quite widely from those measured using the aerosol-probe system. At low engine powers and due to nucleation, gas-probe EIn and EIm values were typically higher than particle probe values. The reverse was true at high engine powers. The relatively smooth, log-normally shaped size distributions measured downstream of the particle probe, when contrasted with the rather messy spectra seen when using the gas probe, seem to justify the added expense and complexity of deploying the specially designed particle probes.

The preceding discussion highlights the point that measured particle emissions indices are highly sensitive to the details of sample collection and dilution. To establish the acceptable range of dilutions, repeated particle characterization measurements were made on samples drawn from the 1-m probe as dry $N_2$-to-sample-air ratios were varied from 6 to 93. Results of the study indicate that EIn values are relatively constant at dilutions greater than 10, but somewhat suppressed at lower values. This is likely caused by enhanced particle coagulation in the less dilute cases. EIm exhibited the opposite trend, reaching a maximum at low dilutions. Although it appeared that dilution ratios of 20 to 30 would have produced the most repeatable measurements of particle-intensive parameters, for practical reasons such as instrument pressure and sensitivity limitations, dilution ratios were maintained in the 8 to 13 range for most of the experiment [15].

APEX measurement team members provided duplicate measurements of important gas-phase species and aerosol parameters to ensure measurement accuracy and minimize potential systematic interferences. Analyses to assess the relative agreement between these measurements are included within a number of companion papers. Aerodyne Research Inc. (ARI) researchers compared TILDAS, PTR-MS, and CGA measurements of numerous gas-phase species and found that the data are, with few exceptions, in good agreement [12,13]. University of Missouri–Rolla (UMR) investigators compared DMS-derived extensive and intensive aerosol parameters with those determined with more conventional (i.e., CPCs and SMPS) instruments. As described by Lobo et al. [15], they found relatively good agreement between geometric mean diameter and geometric standard deviation measurements provided by the various techniques, but some small systematic differences in higher moment-shape parameters and EIn. Onasch et al. [16] found that the sum of MAAP- and AMS-derived mass concentrations are consistent with total aerosol volume concentrations values derived from SMPS size distributions.

## IV. Conclusions

As our understanding of trace-gas species and particle emissions improves, a great number of scientific questions and engineering challenges arise. More specifically, we note that critical research efforts are required to develop an optimal particle sampling methodology by obtaining detailed knowledge of particle evolution within sampling systems and exhaust plumes and to acquire thorough knowledge of the links between particle emissions and fuel composition, combustor and engine design, and engine operation.

## References

[1] Leary, N., *Aviation and the Global Atmosphere*, Cambridge Univ. Press, Cambridge, England, U.K., 1999.

[2] Belvins, L. G., "Particulate Matter Emitted from Aircraft Engines," AIAA International Air and Space Symposium and Exposition: The Next 100 Years, AIAA Paper 2003-2764, July 2003.

[3] Howard, R. P., Wormhoudt, J. C., and Whitefield, P. D., "Experimental Characterization of Gas Turbine Emissions at Simulated Flight Altitude Conditions," Arnold Engineering Development Center, Rept. TR-96-3, Arnold AFB, TN, 1996.

[4] Toon, O. B., and Miake-Lye, R. C., "Subsonic Aircraft: Contrail and Cloud Effects Special Study (SUCCESS)," *Geophysical Research Letters*, Vol. 25, No. 8, 1996, pp. 1109–1112.

[5] Wey, C. C., "Engine Gaseous, Aerosol Precursor and Particulate at Simulated Flight Altitude Conditions," NASA TM 1998-208509, 1998; also U.S. Army Research Lab. Rept. TR-1804, 1998.

[6] Anderson, B., Cofer, W. R., III, and McDougal, D. S., "Air Force F-16 Aircraft Engine Aerosol Emissions Under Cruise Altitude Conditions," NASA TM-1999-209102, 1999.

[7] Anderson, B. E., "An Overview of the NASA Experiment to Characterize Aircraft Volatile Aerosol and Trace-Species Emissions (EXCAVATE)," NASA TM-2005-19019, 2005.

[8] Wey, C. C., Anderson, B. E., Hudgins, C., Wey, C., Li-Jones, X., Winstead, E., Thornhill, L. K., Lobo, P., Hagen, D., Whitefield, P., Yelvington, P. E., Herndon, S. C., Onasch, T. B., Miake-Lye, R. C., Wormhoudt, J., Knighton, W. B., Howard, R., Bryant, D., Corporan, E., Moses, C., Holve, D., and Dodds, W., "Aircraft Particle Emissions Experiment (APEX)," NASA TM 2006-214382, 2006; also U.S. Army Research Lab. Rept. TR-3903, 2006.

[9] Baughcum, S. L., Henderson, S. C., and Tritz, T. G., "Scheduled Civil Aircraft Emission Inventories for 1992: Database Development and Analysis," NASA CR-4700, 1996.

[10] Moses, C. A., "Fuel Technology Support for NASA APEX," NASA TM2006-214382, Appendix B, 2006, pp. 291–306.

[11] Wey, C., and Wey, C. C., "Gas Phase Emissions Measurements During the APEX," NASA TM2006-214382, Appendix C, 2006, pp. 307–348.

[12] Wormhoudt, J., Herndon, S. C., Yelvington, P. E., Miake-Lye, R. C., and Wey, C., "Nitrogen Oxide (NO/NO2/HONO) Emissions Measurements in Aircraft Exhausts," NASA TM2006-214382, Appendix E, 2006, pp. 367–380.

[13] Knighton, W. B., Rogers, T. M., Anderson, B. E., Herndon, S. C., Yelvington, P. E., and Miake-Lye, R. C., "Application of Proton Transfer Reaction Mass Spectrometry (PTR-MS) to Measurement of Volatile Organic Trace Gas Emissions from Aircraft," NASA TM2006-214382, Appendix G, 2006, pp. 397–414.

[14] Anderson, B. E., Winstead, E. L., Hudgins, C. H., and Thornhill, K. L., "Formation of Secondary Particles in Aircraft Exhaust Plumes," NASA TM-2006-214382 Appendix H, 2006, pp. 415–446.

[15] Lobo, P., Hagen, D. E., and Whitefield, P. D., "Physical Characterization of Aerosol Emissions from a Commercial Gas Turbine Engine: Project APEX," NASA TM-2006-214382 Appendix I, 2006, pp. 447–472.

[16] Onash, T. B., Jayne, J., Herndon, S. C., Mortiner, P., Worsnop, D., and Miake-Lye, R. C., "Chemical Properties of Aircraft Engine Exhaust Aerosols Sampled During APEX," NASA TM-2006-214382 Appendix J, 2006, pp. 475–500.

[17] *ICAO Aircraft Engine Emissions Databank* [online database], http://www.caa.co.uk/default.aspx?categoryid=702&pagetype=90 [retrieved 23 July 2007].

L. Maurice
*Associate Editor*